Antigen-presenting intratumoral B cells affect CD4+ TIL phenotypes in non-small cell lung cancer patients

Tullia C. Bruno[1,†], **Peggy J. Ebner**[1], **Brandon L. Moore**[1], **Olivia G. Squalls**[1], **Katherine A. Waugh**[1], **Evgeniy B. Eruslanov**[2], **Sunil Singhal**[2], **John D. Mitchell**[3], **Wilbur A. Franklin**[4], **Daniel T. Merrick**[4], **Martin D. McCarter**[3], **Brent E. Palmer**[5], **Jeffrey A. Kern**[6], and **Jill E. Slansky**[1]

[1]Department of Immunology and Microbiology, University of Colorado School of Medicine, Aurora, CO

[2]Division of Thoracic Surgery, University of Pennsylvania, Philadelphia, PA

[3]Department of Surgery, University of Colorado School of Medicine, Aurora, CO

[4]Department of Pathology, University of Colorado School of Medicine, Aurora, CO

[5]Division of Allergy and Clinical Immunology, University of Colorado School of Medicine, Aurora, CO

[6]Division of Oncology, National Jewish Health, Denver, CO

Abstract

Effective immunotherapy options for patients with non-small cell lung cancer (NSCLC) are becoming increasingly available. The immunotherapy focus has been on tumor infiltrating T cells (TILs); however, tumor infiltrating B cells (TIL-Bs) have also been reported to correlate with NSCLC patient survival. The function of TIL-Bs in human cancer has been understudied, with little focus on their role as antigen-presenting cells and their influence on CD4+ TILs. Compared to other immune subsets detected in freshly isolated primary tumors from NSCLC patients, we observed increased numbers of intratumoral B cells relative to B cells from tumor-adjacent tissues. Furthermore, we demonstrated that TIL-Bs can efficiently present antigen to CD4+ TILs and alter the CD4+ TIL phenotype using an *in vitro* antigen-presentation assay. Specifically, we identified three CD4+ TIL responses to TIL-Bs, which we categorized as: activated, antigen-associated, and non-responsive. Within the activated and antigen-associated CD4+ TIL population, activated TIL-Bs (CD19+CD20+CD69+CD27+CD21+) were associated with an effector T-cell response (IFNγ+ CD4+ TILs). Alternatively, exhausted TIL-Bs (CD19+CD20+CD69+CD27−CD21−) were associated with a regulatory T-cell phenotype (FoxP3+ CD4+ TILs). Our results demonstrate a new role for TIL-Bs in NSCLC tumors in their interplay with CD4+ TILs in the tumor microenvironment, establishing them as a potential therapeutic target in NSCLC immunotherapy.

Corresponding Author: Jill E. Slansky, 12800 East 19th Avenue, Aurora CO 80045, Phone: 303-724-8665, Fax: 303-724-8733, jill.slansky@ucdenver.edu.
†Current address: Department of Immunology, University of Pittsburgh, Pittsburgh, PA.

The authors declare no potential conflicts of interest.

Keywords

TIL-Bs; CD4$^+$ TILs; antigen presentation; NSCLC

Introduction

The goal of cancer immunotherapy is to use the immune system to target cancer cells without harming normal cells; for example, kill cancer cells but not lung epithelial cells in non-small cell lung cancer (NSCLC) patients. Vaccination with tumor-specific antigens and blockade of the inhibitory PD-1:PD-L1 pathway on CD8$^+$ and CD4$^+$ TILs (1–11) have increased survival in lung cancer patients. Despite these successes, only 20–40% of lung cancer patients respond to the current immunotherapies (7–11), suggesting that targeting of other immune cells in NSCLC patients may lead to increased responses. Here, we address the contribution of TIL-Bs to the immune response in these primary tumors.

Similar to CD8$^+$ and effector CD4$^+$ TILs, TIL-Bs positively correlate with overall survival in several solid tumors, including NSCLC (12–19). In addition, TIL-Bs are organized in tertiary lymphoid structures (TLS) with CD4$^+$ TILs, and these structures also positively correlate with survival in NSCLC (18–19). These correlations suggest an antitumor role for TIL-Bs in NSCLC; however, there is still controversy as to whether or not TIL-Bs have an anti- or pro-tumor role in the tumor microenvironment.

In addition to correlating with survival, TIL-Bs generate antitumor antibodies (19–23). Germain et al. demonstrated that germinal center somatic hypermutation and class switch recombination machineries are activated in TIL-Bs from NSCLC patient tumors (19). Further, approximately 50% of patient samples tested have antibody reactivity to tumor antigens (19). It has also been suggested in murine models that TIL-Bs generate antitumor cytokines, directly kill tumor cells, and present tumor antigens (24–31). Antigen presentation is an important function of B cells. Activated B cells from control donor peripheral blood lymphocytes (PBL) present antigens to CD4$^+$ and CD8$^+$ T cells (27,29). Autoimmunity and allograft rejection studies describe the importance of B cells in the formation of TLS and in presentation of auto- or allo-antigens that ultimately influence the CD4$^+$ T-cell phenotype (25, 29–31). TIL-Bs may also present antigens more effectively than tumor dendritic cells (DCs), due to selective presentation of cognate antigen through surface Ig molecules. It is currently hypothesized that CD4$^+$ and CD8$^+$ TILs are primed by DCs in the lymph node and then TIL-Bs elicit a recall response in the tumor. Thus, TIL-Bs serve as a local antigen-presenting cell (APC) by providing secondary stimulation to CD4$^+$ TILs, ultimately increasing their survival and proliferation, which is similar to what occurs in chronic viral infection (32–33).

However, TIL-Bs have also been reported to have a protumor function. TIL-Bs can suppress the antitumor immune response and the tumor microenvironment can promote TIL-B dysfunction. The most prevalent TIL-B–mediated immunosuppression is secretion of IL10 by regulatory B cells (Bregs) (35–39). In NSCLC patients, the frequency and absolute number of IL10-producing Bregs is elevated and positively associated with advanced clinical

stage (37). Further, Bregs can secrete IL35 and TGFβ, which can also suppress the immune response (40–42).

There is also evidence for B cell–mediated immunoregulation in addition to Bregs. In autoimmunity and autograft rejection, removal of B cells from TLS results in decreased T-cell function, and B cells (specifically Bregs) can skew the population toward a Treg phenotype (25, 30–31,39). In cancer, B cells can convert CD4+CD25− T cells into Tregs when cocultured with tongue squamous cell carcinoma cell lines (39). Within this same study, Zhou et al. demonstrated that IL10+ TIL-Bs positively correlated with increased Tregs and decreased survival. B cell–mediated immunoregulation has also been shown using B and T cells isolated from the ascites of ovarian cancer patients (38). However, studies of TIL-Bs from NSCLC patients have not yet been published.

Based on preliminary studies of TIL-Bs in NSCLC patients, we hypothesized that TIL-Bs present antigen to CD4+ TILs and promote a prolonged antitumor immune response. However, given the evidence for B-cell exhaustion in the context of chronic antigen exposure (43–44), we also hypothesized that B cells may be exhausted in some NSCLC patients. To test these hypotheses, we compared TIL-Bs to other immune cell subsets that infiltrated primary NSCLC tumors. We also assessed the function of TIL-Bs as APCs in the tumor microenvironment. To further assess TIL-B–mediated immunoregulation of an anti- or protumor CD4+ TIL response, we analyzed the association of an activated or exhausted TIL-B phenotype with the proportion of CD4+ Th1 cells and Tregs. Our results show that B cells are increased at the site of the tumor relative to tumor-adjacent tissues and have variable function as APCs in NSCLC. In addition, we demonstrate that the activated or exhausted TIL-B phenotype predicts the CD4+ TIL phenotype.

Materials and Methods

Patient tissues

All NSCLC tissues were acquired under a University of Colorado Anschutz Medical Campus and National Jewish Health Institutional Review Board (IRB)-approved protocol with written informed consent obtained from each patient in conjunction with the University of Colorado Lung Cancer SPORE. There were no restrictions on cancer subtype, smoking status, age, race, or prior adjuvant therapy; patients were segregated by tumor subtype after final histological analysis. Control donor PBLs were collected through a material transfer agreement with Bonfils Blood Donation Center (Denver, CO). Disease-free control lung tissue was collected through an IRB-approved protocol at National Jewish Health. Control splenocytes and untreated HIV+ PBLs were collected through an IRB-approval protocol at the University of Colorado. NSCLC pleural effusions and additional NSCLC primary tumors were provided through collaboration at the University of Pittsburgh and the University of Pennsylvania or through an IRB-approved protocol with the National Disease Research Interchange. All patient demographics are summarized in Table 1.

Sample processing and lymphocyte selection

Patient-matched PBL samples were collected by venipuncture into 10 ml whole blood tubes with heparin solution (BD Biosciences Vacutainer Systems) the day or week prior to surgery, and lymphocytes were enriched using a Ficoll gradient (GE Healthcare). Tumor and tumor adjacent tissue in each patient specimen was identified by University of Colorado pathologists. Gross identification of the tumor was performed and tumor adjacent tissue was procured at the farthest distance from the tumor allowed by surgical margins. Within 1 h of resection, lung tumor and tumor-adjacent tissue were mechanically disrupted and incubated with the enzyme Liberase DL (Roche, 50 μg/ml) for 25 min at 37°C to facilitate the release of lymphocytes from tissue. After the incubation, the tissue was passed through a 100-micron filter to obtain a single-cell suspension. Cells were resuspended in complete medium (RPMI 1640 medium supplemented with 1% L-glutamatine, 1% nonessential amino acids, 1% sodium pyruvate, 1% penicillin-streptomycin, and 10% FCS) for counting. Cells were evenly distributed for cell staining and/or resuspended in 1 ml of Dynal buffer for cell separation (PBS supplemented with 25% BSA). B cells and T cells were positively isolated using the Dynal CD19, CD8 or CD4 Positive Isolation Kit (Invitrogen) and the manufacturer's recommended protocol, including magnetic bead detachment. Positively isolated cells were counted and used for functional assays. Using directly conjugated monoclonal antibodies against CD19, CD8, CD4 and CD3 (clones HIB19, RPA-T8, RPA-T4, and HIT3a, respectively, Biolegend), approximately 1,000 cells from each patient were stained and analyzed by flow cytometry to verify >90% purity of positively isolated B and T cells.

Isolation of CD11c+ myeloid cells

CD11c+ myeloid cells were isolated by culturing single-cell suspensions for 2 h at 37°C for adherence to the culture plate. Subsequently, adherent cells were stimulated for 24 h with LPS (100 ng/ml, Sigma) and harvested the next day for an *in vitro* AP assay. Prior to the assay, cells were analyzed with monoclonal antibodies to CD11c, HLA-DR, and CD86 (clones 3.9, L243, and IT2.2, respectively, Biolegend) to verify mature CD11c+ myeloid cells.

Antibody staining and flow cytometry

Single cell suspensions of tumor and tumor-adjacent tissue were stained with surface antibodies for CD19, CD20, CD3, CD8, CD4, CD56 and CD11c (clones HIB19, 2H7, HIT3a, RPA-T8, RPA-T4, HCD56, and 3.9, respectively, Biolegend) and an intracellular stain for the transcription factor FoxP3 (clone PCH101, Ebioscence) for Figure 1 and for CD19, CD20, CD21, CD69, CD27 and HLA-DR (clones HIB19, 2H7, HB5, FN50, O323, and L243, respectively, Biolegend and Ebioscence) for Figs. 2 and 3. Positive and negative controls for staining were PBLs from patients or control donors, lymphocytes from control donor spleens, lymphocytes from control (disease-free) lungs, lymphocytes from NSCLC pleural metastases, and PBL from untreated, HIV+ patients. Flow cytometry was conducted using an LSR II (BD Biosciences) and data were analyzed using FlowJo software (Tree Star, Inc.). For Fig. 2B, total lymphocyte infiltration was calculated using the following equation:

[Total cell number from tissue X % lymphocyte gate X % lymphocyte population, i.e. CD19$^+$]/ [mass of tissue in grams].

Antigen presentation (AP) assay

CD4$^+$ T cells, B cells, and DCs were selected from the indicated tissues. CD4$^+$ T cells were labeled with CFSE and cocultured at an equivalent ratio with B cells or DCs ± the indicated protein ± costimulation with anti-CD40 (clone 5C3, 4 μg/ml, Biolegend) and anti-CD28 (clone CD28.2, 1 μg/ml, Ebioscience). Anti-HLA-DR, DP, DQ was utilized to block MHC class II antigen presentation (clone Tu39, 1 μg/ml, BD Biosciences). CD4$^+$ T cells were left unstimulated for a negative control and were activated with plate bound anti-CD3 (clone OKT3, 0.5 μg/ml, Ebioscience) and soluble anti-CD28 (1 μg/ml) as a positive control for proliferation and intracellular protein staining. Control PBL donors with increased exhausted B cells (solid triangles) were rested for 2d *in vitro* without stimulation to decrease CD21 and CD27 expression. Control PBL donors with increased activated B cells (open triangles) were used *ex vivo*. The cells were cocultured for 5 d and were then harvested and restimulated for 4–6 h *in vitro* with PMA (0.1 μM, Sigma) and ionomycin (0.5 mM, Sigma) plus BD Golgistop (Monensin, BD recommended concentration) for intracellular cytokine analysis. Cell division was analyzed by CFSE dilution and Ki67 nuclear protein. Ki67, IFNγ, and FoxP3 expression (clones Ki-67, 4S.B3 and PCH101, respectively, Biolegend and Ebioscience) was detected using a nuclear intracellular staining kit (FoxP3 staining kit, Ebioscience). Flow cytometry was performed as above.

Generation of cell lysates and purified XAGE-1b protein

NSCLC patient tumor lysates were generated by two freeze/thaw cycles followed by sonication. EBV lysates were prepared by 0.45 μm filtration of B95-8 EBV cell line supernatant and freeze/thaw lysate. XAGE-1b protein was purified utilizing a previously described method (34).

Statistical Analysis

All statistical analyses were performed using GraphPad Prism 6.0. *In vitro* experiments were repeated at least three times for statistical significance. P 0.05 was considered statistically significant and statistical differences were measured as follows: Fig. 1B, Fig. 2B, Fig. 4B/E, and Fig. 5B used the paired, one-sided Student t test, and Fig. 3A, Fig. 4A and Fig. 6C used the unpaired, one-sided Student t test.

Results

B cells are increased in the tumors of NSCLC patients

To define the role of TIL-Bs in human NSCLC, we first performed a comprehensive quantification of intratumoral TILs compared to lymphocytes in tumor-adjacent tissue using flow cytometric analyses. TIL-Bs were increased in frequency and total number compared to tumor-adjacent tissue in all subtypes of NSCLC, but most prominently in adenocarcinomas (Fig. 1A and B). To understand how the B-cell density in tissues from NSCLC patients compares to other tissues, we also examined the frequency of B cells from PBL of NSCLC patients and lung, PBL and spleen of control donors (Fig. 1B). Next, we used other

lymphocyte markers to compare the frequency of B cells in the tumor and tumor-adjacent tissues to other lymphocyte subsets. The total number of TIL-Bs in the tumor was increased relative to other TILs, but were similar in numbers to intratumoral Tregs (Fig. 2A and B). Whereas Tregs have been well studied in NSCLC patients (45), TIL-Bs have been understudied. Thus, since we observed an increase of TIL-Bs in NSCLC tumors, we assayed their function as an APC.

TIL-Bs presented antigen to CD4^{+} TILs

We first established an *in vitro* assay to test B cells for antigen presentation (AP). Utilizing healthy donor splenocytes, B cells were cocultured with CFSE-labeled T cells and T-cell proliferation measured as a marker of successful antigen presentation. As expected, CD4^{+} T cells from control PBL divided in the presence of B cells with EBV lysates, but not in the presence of EBV lysates and an MHC class II blocking antibody (Fig. 3A/B). In addition, antigen presentation by B cells was similar to CD11c^{+} myeloid cells in this assay (Fig. 3A).

Next, we examined the expression of antigen presenting molecules, MHC class II (HLA-DR) on TIL-Bs. Most TIL-Bs expressed MHC class II, although at lower levels than in B cells from control, healthy donor spleen (Fig. 4A). We compared TIL-Bs to other intratumoral CD11c^{+} myeloid cells, which are potent APCs. Although the density of B cells in the tumor relative to the tumor-adjacent tissue increased more than the density of CD11c^{+} myeloid cells (Fig. 2B), there were similar total numbers of intratumoral TIL-Bs and CD11c^{+} myeloid cells in NSCLC (Fig. 4B). Because these findings suggested an APC function for TIL-Bs, we utilized the AP assay to determine if TIL-Bs present antigen to CD4^{+} TILs in NSCLC patients. As with cells from healthy donor splenocytes, CD4^{+} T cells divided in the presence of B cells with EBV lysate (Fig. 4C). Further, we tested if patient-derived autologous tumor lysate and a purified cancer-testis protein, XAGE-1b, were presented by TIL-Bs to CD4^{+} TILs. We identified three types of CD4^{+} TIL responses: activated responses, antigen-associated responses, and no responses. Activation of some CD4^{+} TIL responses did not require exogenous antigen, just the addition of TIL-Bs (Fig. 4D, purple). Antigen-associated CD4^{+} TIL responses occurred when exogenous antigen was added to the TIL-B coculture (Fig. 4D/E, green). In this group, CD4^{+} TILs responded to addition of EBV lysate, autologous tumor lysate, and purified XAGE-1b protein. Lastly, there were patients with no CD4^{+} TIL responses regardless of addition of TIL-Bs alone or TIL-Bs with exogenous antigen (Fig. 4D/E, blue).

Exhausted and activated TIL-B phenotypes found in NSCLC patients

We analyzed B-cell exhaustion as one mechanism to explain CD4^{+} TIL non-responsiveness to TIL-B antigen presentation. B-cell exhaustion was first described in the tonsils of HIV^{+} patients as a memory population of B cells with downregulation of CD21 and CD27 (43–44). In some studies, there is evidence of decreased function and increased inhibitory receptors on exhausted B cells; however, the phenotype is still being defined. We used untreated HIV^{+} PBL as a positive control for downregulation of CD27 and CD21 on CD69^{+} B cells and NSCLC pleural metastases as a positive control for upregulation of CD27 and CD21 on CD69^{+} B cells. We also utilized control PBLs to demonstrate CD21 and CD27 expression on B cells *ex vivo* from adult donors (Fig. 5A). We identified both activated

(CD69$^+$HLA$^-$DR$^+$CD27$^+$CD21$^+$) and exhausted (CD69$^+$HLA$^-$DR$^+$CD27$^-$CD21$^-$) TIL-B phenotypes in NSCLC tumors; however, NSCLC patient tumors had more activated than exhausted TIL-Bs (Fig. 5B).

TIL-B phenotype associates with CD4$^+$ TIL phenotype

Because we observed both activated and exhausted TIL-Bs in NSCLC and a preferential expansion of CD4$^+$ TILs over CD8$^+$ TILs in AP assays (Fig. 6A), we queried whether TIL-Bs associated with a particular CD4$^+$ TIL phenotype. To determine whether the TIL-B phenotype correlated with the CD4$^+$ TIL phenotype, the TIL-B exhaustion profile prior to the AP assay was analyzed with the final CD4$^+$ TIL phenotype at the end of our AP assay. Tregs were identified as CD4$^+$FoxP3$^+$IFNγ^- and Th1 cells were identified as CD4$^+$FoxP3$^-$ IFNγ^+ (Fig. 6B). B cells from control donors that had induced B-cell exhaustion and exhausted TIL-Bs from NSCLC patients correlated with increased Tregs at the end of the AP assay (Fig. 6C). Conversely, B cells from control donors that had activated B cells and activated TIL-Bs from NSCLC patients correlated with increased Th1 CD4$^+$ TILs at the end of the AP assay (Fig. 6C). Finally, we examined the disease status of the small cohort of patients that had follow-up data from the start of the study. Patients with TIL-Bs that did not efficiently present antigen either had relapsed disease or were deceased ($n = 4$, Table 1). In contrast, the patients that had either activated or antigen-associated CD4$^+$ TIL responses remained tumor-free. These results suggest the hypothesis that some NSCLC patients have a more activated tumor microenvironment and TIL-B antigen presentation, which may contribute to the overall quality of the immune response in NSCLC patients. However, further investigation and more patient samples are required to confirm these findings.

Discussion

Conclusions regarding the function of TIL-Bs in human cancer are usually either anti- and protumor, depending on the study. However, in NSCLC patients, evidence suggests an antitumor role for TIL-Bs. TIL-Bs generate antibodies to tumors, and detection of TIL-Bs and TLS correlate with better prognosis. Despite these reports, comprehensive studies on the association of TIL-Bs with other immune subsets had not been completed and TIL-Bs had not been thoroughly studied as APCs in NSCLC patients. Further, many studies on the immune contexture in primary NSCLC tumors are done in histological sections, not in fresh, *ex vivo* tissue. Finally, most functional studies that describe TIL-B-mediated antigen presentation or immunoregulation are not performed utilizing TIL-Bs from the patient primary tumor, but rather, murine or in vitro culture models.

Our data fill the gaps described above and provide two observations about TIL-Bs in NSCLC patients. First, we demonstrated that TIL-Bs can present antigen to CD4$^+$ TILs in some NSCLC patients. Second, we determined that the TIL-B phenotype, activated or exhausted, associates with the CD4$^+$ TIL phenotype. Consequently, we suggest a two-pronged model for TIL-B function in NSCLC patients. In the antigen presentation part of the model TIL-Bs can present endogenous tumor antigens to CD4$^+$ TILs spontaneously (activated responses) or after re-stimulation with antigen (antigen-associated responses) or not at all (no responses). In the immunoregulation part of the model, the CD4$^+$ TIL

phenotype can be predicted by the prevalence of TIL-B exhaustion or activation markers. Thus, the TIL-B phenotype influences the CD4^{+} TIL phenotype, which may determine if downstream cytolytic CD8^{+} TIL responses are further activated or suppressed in NSCLC patients.

To understand this two-pronged model of TIL-B function, we first considered the two modalities for TIL-B function. The "B cell-intrinsic model" suggests recruitment of TIL-Bs to the tumor by IFNγ produced by T cells. TIL-Bs in this model do not form TLS with CD4^{+} TILs and suppress antitumor function via the secretion of the suppressive cytokines IL10 and IL35 (30, 35–42). This intrinsic model does not support our data on antigen presentation and immunoregulation as both of these functions require cell-to-cell contact. In contrast, the "B cell-extrinsic model" suggests that TIL-Bs are recruited to the tumor site and form TLS with CD4^{+} TILs to influence the overall immune response (30). Our hypothesis that TIL-Bs present antigen to CD4^{+} TILs and promote an antitumor immune response supports the extrinsic model of TIL-B function. Our hypothesis was supported by the observation of TIL-Bs presenting antigen to CD4^{+} TILs in NSCLC patients. Support for antigen-specific TIL-B responses have been described in two ways in NSCLC patients: (1) tumor-specific antibody production and (2) oligoclonality of TIL-Bs in TLS. Further, in studies with mice that receive an antigenic vaccination, B cells enhance the response to vaccine (30). Our data combined with these other studies provide evidence for a B-cell extrinsic role in NSCLC patients. It remains unclear why TIL-Bs from some patients do not present antigen to CD4^{+} TILs. Perhaps the TIL-Bs pick up but do not properly process antigen. Or, perhaps TIL-Bs are anergized by other components of the tumor microenvironment.

The second portion of our hypothesis that is supported by the B cell-extrinsic model relates to TIL-B-mediated immunoregulation of CD4^{+} TILs. In line with our hypothesis, we observed an exhausted TIL-B phenotype in our NSCLC patients. However, the function of these exhausted TIL-Bs does not fit with the definition of lymphocyte exhaustion as described in models of chronic infection or cancer. In these models, T cells and B cells that are exhausted are described as less functional. Such T cells proliferate less and produce less cytokine (46–48); B cells produce less antibody (43–44). The TIL-Bs in our NSCLC patient samples with an exhausted signature still present antigen. However, they also associate with CD4^{+} T cells of a Treg phenotype. One consideration in understanding the TIL-B exhaustion profile in NSCLC patients is control of host damage during chronic antigen exposure. In chronic infection and autoimmunity, B cells may attenuate T-cell responses in an attempt to decrease host damage. It is possible that in the context of chronic self-antigen, such as in tumors, TIL-Bs may obtain an exhausted phenotype to skew the CD4^{+} TILs to a Treg population for this purpose, ultimately dampening the overall antitumor response in the tumor. B cell-mediated immunoregulation has been implicated in various malignancies. However, the phenotypic markers of activated and exhausted TIL-Bs must be enhanced to better understand how they differ from Breg populations that dampen the immune response by secretion of suppressive cytokines. Location may contribute to the difference between Bregs and exhausted TIL-Bs: IL10 producing Bregs may be scattered throughout the tumor whereas exhausted TIL-Bs may be found in TLS.

Our data suggest strategies to target TIL-Bs in NSCLC patients to improve patient responses to immunotherapy. Total B-cell depletion has little clinical benefit in patients with solid tumors (49–50); here we suggest that targeting a specific subtype of TIL-B is necessary for effective immunotherapies. Focusing ablation on B cells with an exhausted phenotype may reduce promotion of the Treg phenotype resulting in reduced tumor growth. In addition, the link between tumor-specific antibodies and the tumor antigens that are processed and presented by TIL-Bs could be targeted TIL-B-based immunotherapies. TIL-Bs in NSCLC are often in TLS, which suggests an antigen-specific role for TIL-Bs. We observe TLS in our patient samples, and they have been reported in NSCLC patients by other groups (18–19). However, whether the tumor antigens that are targeted by TIL-B antibodies can also be processed and presented to CD4$^+$ TILs is unknown. If so, this strategy would link cellular and humoral immunity in solid tumors. Finally, an increased understanding of the activated and exhausted TIL-B phenotypes may be reflective of an immunological biomarker to measure the quality of the immune response in NSCLC patients that are being considered for immunotherapy.

These studies may improve patient responses to immunotherapy in two ways: (1) increased antigen presentation by TIL-Bs to CD4$^+$ TILs in the tumor microenvironment in combination with anti–PD-1 therapy, may further increase tumor-specific immune responses and (2) methods to skew exhausted B cells to activated B cells or to deplete exhausted TIL-Bs may promote an activated, antitumor microenvironment in NSCLC patients. An activated microenvironment offers an advantage in obtaining a productive response to immunotherapy. Thus, by targeting TIL-Bs in combination with current immunotherapies, we can further improve NSCLC patient survival.

Acknowledgments

References

1. Hanibuchi M, Yano S, Nishioka Y, Yanagawa H, Miki T, Sone S. Immunological circumvention of multiple organ metastases of multidrug resistant human small cell lung cancer cells by mouse-human chimeric anti-ganglioside GM2 antibody KM966. Clin Exp Metastasis. 2000; 18(5):353–60. [PubMed: 11467766]

2. Lara PN Jr, Laptalo L, Longmate J, Lau DH, Gandour-Edwards R, Gumerlock PH, et al. Trastuzumab plus docetaxel in HER2/neu-positive non-small-cell lung cancer: a California Cancer Consortium screening and phase II trial. Clin Lung Cancer. 2004; 5(4):231–6. [PubMed: 14967075]

3. Vuillez JP, Kraeber-Bodéré F, Moro D, Bardiès M, Douillard JY, Gautherot E, et al. Radioimmunotherapy of small cell lung carcinoma with the two-step method using a bispecific anti-carcinoembryonic antigen/anti-diethylenetriaminepentaacetic acid (DTPA) antibody and iodine-131

Di-DTPA hapten: results of a phase I/II trial. Clin Cancer Res. 1999; 5(10 Suppl):3259s–3267s. [PubMed: 10541373]

4. Du N, Li X, Li F, Zhao H, Fan Z, Ma J, et al. Intrapleural combination therapy with bevacizumab and cisplatin for non-small cell lung cancermediated malignant pleural effusion. Oncol Rep. 2013

5. Wang Y, Deng G, Liu X, Cho WC. Monoclonal antibodies in lung cancer. Expert Opin Biol Ther. 2013; 13(2):209–26. [PubMed: 23240766]

6. Brahmer JR, Drake CG, Wollner I, Powderly JD, Picus J, Sharfman WH, et al. Phase I study of single-agent anti-programmed death-1 (MDX-1106) in refractory solid tumors: safety, clinical activity, pharmacodynamics, and immunologic correlates. J Clin Oncol. 2010; 28(19):3167–75. [PubMed: 20516446]

7. Giri A, Walia SS, Gajra A. Clinical Trials Investigating Immune Checkpoint Inhibitors in Non-Small-Cell Lung Cancer. Rev Recent Clin Trials. 2016 Jul 24. Epub ahead of print.

8. Qin A, Coffey DG, Warren EH, Ramnath N. Mechanisms of immune evasion and current status of checkpoint inhibitors in non-small cell lung cancer. Cancer Med. 2016; 5(9):2567–78. [PubMed: 27416962]

9. Morgensztern D, Herbst RS. Nivolumab and Pembrolizumab for Non-Small Cell Lung Cancer. Clin Cancer Res. 2016; 22(15):3713–7. [PubMed: 27252413]

10. Brahmer J, Reckamp KL, Baas P, Crinò L, Eberhardt WE, Poddubskaya E, et al. Nivolumab versus Docetaxel in Advanced Squamous-Cell Non-Small-Cell Lung Cancer. N Engl J Med. 2015; 373(2):123–35. [PubMed: 26028407]

11. Garon EB, Rizvi NA, Hui R, Leighl N, Balmanoukian AS, Eder JP, et al. Pembrolizumab for the treatment of non-small-cell lung cancer. N Engl J Med. 2015; 372(21):2018–28. [PubMed: 25891174]

12. Al-Shibli KI, Donnem T, Al-Saad S, Persson M, Bremnes RM, Busund LT. Prognostic effect of epithelial and stromal lymphocyte infiltration in non-small cell lung cancer. Clin Cancer Res. 2008; 14(16):5220–7. [PubMed: 18698040]

13. Milne K, Köbel M, Kalloger SE, Barnes RO, Gao D, Gilks CB, et al. Systematic analysis of immune infiltrates in high-grade serous ovarian cancer reveals CD20, FoxP3 and TIA-1 as positive prognostic factors. PLoS One. 2009; 4(7):e6412. [PubMed: 19641607]

14. Nedergaard BS, Ladekarl M, Nyengaard JR, Nielsen K. A comparative study of the cellular immune response in patients with stage IB cervical squamous cell carcinoma. Low numbers of several immune cell subtypes are strongly associated with relapse of disease within 5 years. Gynecol Oncol. 2008; 108(1):106–11. [PubMed: 17945335]

15. Woo JR, Liss MA, Muldong MT, Palazzi K, Strasner A, Ammirante M, et al. Tumor infiltrating B-cells are increased in prostate cancer tissue. J Transl Med. 2014; 12(1):30. [PubMed: 24475900]

16. Shi JY, Gao Q, Wang ZC, Zhou J, Wang XY, Min ZH, et al. Margin-infiltrating CD20(+) B cells display an atypical memory phenotype and correlate with favorable prognosis in hepatocellular carcinoma. Clin Cancer Res. 2013; 19(21):5994–6005. [PubMed: 24056784]

17. Shimabukuro-Vornhagen A, Schlößer HA, Gryschok L, Malcher J, Wennhold K, Garcia-Marquez M, et al. Characterization of tumor-associated B-cell subsets in patients with colorectal cancer. Oncotarget. 2014; 5(13):4651–64. [PubMed: 25026291]

18. Dieu-Nosjean MC, Antoine M, Danel C, Heudes D, Wislez M, Poulot V, et al. Long-term survival for patients with non-small-cell lung cancer with intratumoral lymphoid structures. J Clin Oncol. 2008; 26(27):4410–7. [PubMed: 18802153]

19. Germain C, Gnjatic S, Tamzalit F, Knockaert S, Remark R, Goc J, et al. Presence of B cells in tertiary lymphoid structures is associated with a protective immunity in patients with lung cancer. Am J Respir Crit Care Med. 2014; 7(189):832–44.

20. Mizukami M, Hanagiri T, Shigematsu Y, Baba T, Fukuyama T, Nagata Y, et al. Effect of IgG produced by tumor-infiltrating B lymphocytes on lung tumor growth. Anticancer Res. 2006; 26(3A):1827–31. [PubMed: 16827114]

21. Yasuda M, Mizukami M, Hanagiri T, Shigematsu Y, Fukuyama T, Nagata Y, et al. Antigens recognized by IgG derived from tumor-infiltrating B lymphocytes in human lung cancer. Anticancer Res. 2006; 26(5A):3607–11. [PubMed: 17094490]

22. Carmi Y, Spitzer MH, Linde IL, Burt BM, Prestwood TR, Perlman N, et al. Allogeneic IgG combined with dendritic cell stimuli induce antitumour T-cell immunity. Nature. 2015; 521(7550): 99–104. [PubMed: 25924063]

23. Kotlan B, Simsa P, Teillaud JL, Fridman WH, Toth J, McKnight M, et al. Novel ganglioside antigen identified by B cells in human medullary breast carcinomas: the proof of principle concerning the tumor-infiltrating B lymphocytes. J Immunol. 2005; 175:2278–2285. [PubMed: 16081796]

24. Rivera A, Chen CC, Ron N, Dougherty JP, Ron Y. Role of B cells as antigen-presenting cells in vivo revisited: antigen-specific B cells are essential for T cell expansion in lymph nodes and for systemic T cell responses to low antigen concentrations. Int Immunol. 2001; 13(12):1583–1593. [PubMed: 11717199]

25. Nelson BH. CD20+ B cells: the other tumor-infiltrating lymphocytes. J Immunol. 2010; 185(9): 4977–4982. [PubMed: 20962266]

26. Candolfi M, Curtin JF, Yagiz K, Assi H, Wibowo MK, Alzadeh GE, et al. B cells are critical to T-cell-mediated antitumor immunity induced by a combined immune-stimulatory/conditionally cytotoxic therapy for glioblastoma. Neoplasia. 2011; 13(10):947–960. [PubMed: 22028620]

27. Rodríguez-Pinto D. B cells as antigen presenting cells. Cell Immunol. 2005; 238:67–75. [PubMed: 16574086]

28. Haynes NM, Hawkins ED, Li M, McLaughlin NM, Hämmerling GJ, Schwendener R, et al. CD11c + dendritic cells and B cells contribute to the tumoricidal activity of anti-DR5 antibody therapy in established tumors. J Immunol. 2010; 185(1):532–541. [PubMed: 20505139]

29. Yanaba K, Bouaziz JD, Matsushita T, Magro CM, St Clair EW, Tedder TF. B-lymphocyte contributions to human autoimmune disease. Immunol Rev. 2008; 223:284–299. [PubMed: 18613843]

30. Shen M, Sun Q, Wang J, Pan W, Ren X. Positive and negative functions of B lymphocytes in tumors. Oncotarget. 2016 Jun 15.

31. Guy TV, Terry AM, Bolton HA, Hancock DG, Shklovskaya E, Fazekas de StGroth B. Pro- and antitumour effects of B cells and antibodies in cancer: a comparison of clinical studies and preclinical models. Cancer Immunol Immunother. 2016; 65(8):885–96. [PubMed: 27222052]

32. Wakim LM, Waithman J, van Rooijen N, Heath WR, Carbone FR. Dendritic cell-induced memory T cell activation in nonlymphoid tissues. Science. 2008; 319:198–202. [PubMed: 18187654]

33. McGill J, Van Rooijen N, Legge KL. Protective influenza-specific CD8 T cell responses require interactions with dendritic cells in the lungs. J Exp Med. 2008; 205:1635–1646. [PubMed: 18591411]

34. Jordan KR, Buhrman JD, Sprague J, Moore BL, Gao D, Kappler JW, et al. TCR hypervariable regions expressed by T cells that respond to effective tumor vaccines. Cancer Immunol Immunother. 2012; 61(10):1627–38. [PubMed: 22350070]

35. Tedder TF. B10 cells: a functionally defined regulatory B cell subset. J Immunolo. 2015; 194(4): 1395–1401.

36. Chen T, Song D, Min Z, Wang X, Gu Y, Wei B, et al. Perioperative dynamic alterations in peripheral regulatory T and B cells in patients with hepatocellular carcinoma. Journal of translational medicine. 2012; 10:14. [PubMed: 22272696]

37. Liu J, Wang H, Yu Q, Zheng S, Jiang Y, Liu Y, et al. Aberrant frequency of IL-10-producing B cells and its association with Treg and MDSC cells in non-small cell lung carcinoma patients. Human immunology. 2016; 77(1):84–89. [PubMed: 26527508]

38. Wei X, Jin Y, Tian Y, Zhang H, Wu J, Lu W, et al. Regulatory B cells contribute to the impaired antitumor immunity in ovarian cancer patients. Tumour biology. 2016; 37(5):6581–6588. [PubMed: 26638169]

39. Zhou X, Su YX, Lao XM, Liang YJ, Liao GQ. CD19(+)IL-10(+) regulatory B cells affect survival of tongue squamous cell carcinoma patients and induce resting CD4(+) T cells to CD4(+)Foxp3(+) regulatory T cells. Oral oncology. 2016; 53:27–35. [PubMed: 26631955]

40. Zhang Y, Sun H, Wu H, Tan Q, Xiang K. Interleukin 35 is an independent prognostic factor and a therapeutic target for nasopharyngeal carcinoma. Contemporary oncology. 2015; 19(2):120–124. [PubMed: 26034389]

41. Fan YG, Zhai JM, Wang W, Feng B, Yao GL, An YH, et al. IL-35 over-expression is associated with genesis of gastric cancer. Asian Pacific journal of cancer prevention. 2015; 16(7):2845–2849. [PubMed: 25854372]

42. Pylayeva-Gupta Y, Das S, Handler JS, Hajdu CH, Coffre M, Koralov SB, et al. IL35-producing B cells promote the development of pancreatic neoplasia. Cancer discovery. 2016; 6(3):247–255. [PubMed: 26715643]

43. Moir S, Ho J, Malaspina A, Wang W, DiPoto AC, O'Shea MA, et al. Evidence for HIV-associated B cell exhaustion in a dysfunctional memory B cell compartment in HIV-infected viremic individuals. J Exp Med. 2008; 205(8):1797–805. [PubMed: 18625747]

44. Sciaranghella G, Tong N, Mahan AE, Suscovich TJ, Alter G. Decoupling activation and exhaustion of B cells in spontaneous controllers of HIV infection. AIDS. 2013; 27(2):175–80. [PubMed: 23135171]

45. Zhao S, Jiang T, Zhang L, Yang H, Liu X, Jia Y, et al. Clinicopathological and prognostic significance of regulatory T cells in patients with non-small cell lung cancer: A systematic review with meta-analysis. Oncotarget. 2016; 7(24):36065–36073. [PubMed: 27153545]

46. Wherry EJ. T cell exhaustion. Nat Immunol. 2011; 12:492–499. [PubMed: 21739672]

47. Youngblood B, Wherry EJ, Ahmed R. Acquired transcriptional programming in functional and exhausted virus-specific CD8 T cells. Curr Opin HIV AIDS. 2012; 7:50–57. [PubMed: 22134341]

48. Wherry EJ, Ha SJ, Kaech SM, Haining WN, Sarkar S, Kalia V, Subramaniam S, et al. Molecular Signature of CD8+ T Cell Exhaustion during Chronic Viral Infection. Immunity. 2007; 27:670–684. [PubMed: 17950003]

49. Aklilu M, Stadler WM, Markiewicz M, Vogelzang NJ, Mahowald M, Johnson M, et al. Depletion of normal B cells with rituximab as an adjunct to IL-2 therapy for renal cell carcinoma and melanoma. Ann Oncol. 2004; 15(7):1109–1114. [PubMed: 15205206]

50. Barbera-Guillem E, Nelson MB, Barr B, Nyhus JK, May KF Jr, Feng L, et al. B lymphocyte pathology in human colorectal cancer. Experimental and clinical therapeutic effects of partial B cell depletion. Cancer Immunol Immunother. 2000; 48(10):541–549. [PubMed: 10630306]
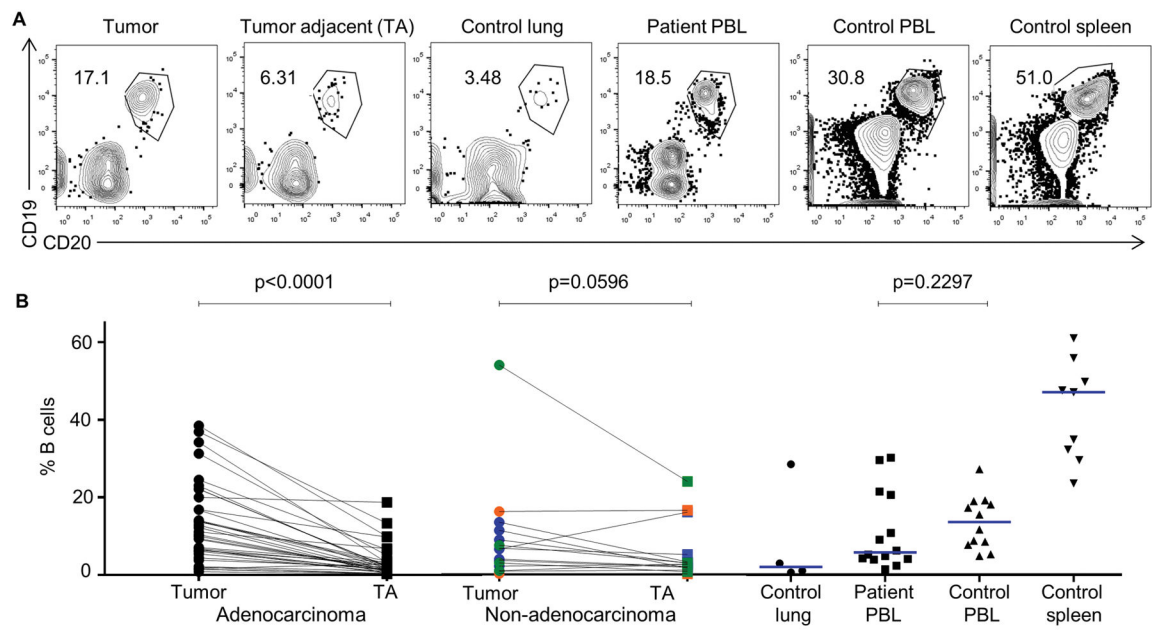
Fig. 1. Frequency and total number of TIL-Bs increase in NSCLC primary tumors
(**A**) Single-cell suspensions of lymphocytes from the indicated tissues were surface stained with anti-CD19 and anti-CD20. (**B**) B-cell frequency of paired tumor and tumor-adjacent tissue is shown: adenocarcinomas (black, $n = 37$, $P < 0.0001$), squamous cell carcinomas (blue, $n = 9$), large cell carcinomas (orange, $n = 2$), and carcinoid tumors (green, $n = 4$), $p = 0.0596$ (non-adenocarcinomas). Relative B cell frequency in other control and patient tissues is shown for comparison.
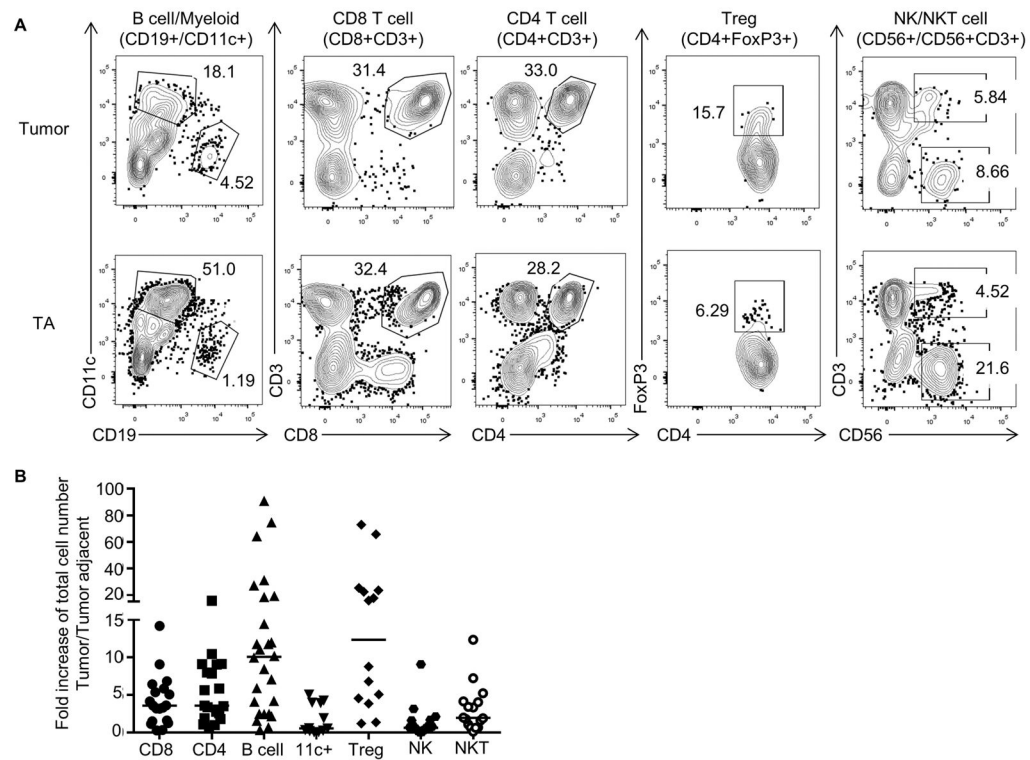
Fig. 2. Total number of TIL-Bs increase in NSCLC tumors compared to other immune subsets
(**A**) Single-cell suspensions were stained with the indicated antibodies; representative flow cytometry plots are shown. (**B**) Using the gating strategy shown in (A), the fold increase of total tumor infiltrating lymphocytes at the site of the tumor compared to tumor-adjacent tissue is shown (bar indicates median value, n = 12–26), p values: TIL-B vs. CD8, P = 0.010, TIL-B vs. CD4, P = 0.014, TIL-B vs. 11c+, P = 0.008, TIL-B vs. Treg, n.s. 11c+ represents myeloid CD11c+ cells.
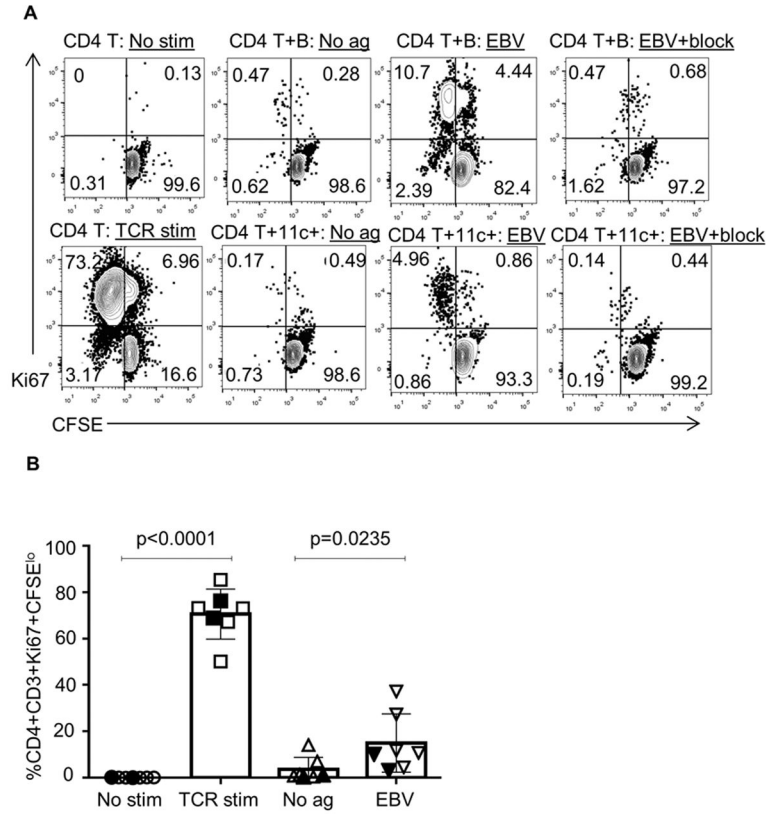
Fig. 3. B cells from healthy donors present antigen to CD4+ T cells *in vitro*
(**A**) In representative AP assays, autologous CD4+ T cells and B cells or DCs from control PBL were cocultured with co-stimulation and EBV lysate or a blocking antibody to HLA class II. The "TCR stim" sample contained plate-bound anti-CD3 and soluble anti-CD28. (**B**) Compiled results (right) from the AP assay ($p = 0.0235$) using control splenocytes (open symbols, $n = 5$) and control PBL (closed symbols, $n = 2$) are shown. 11c+ represents myeloid CD11c+ cells.
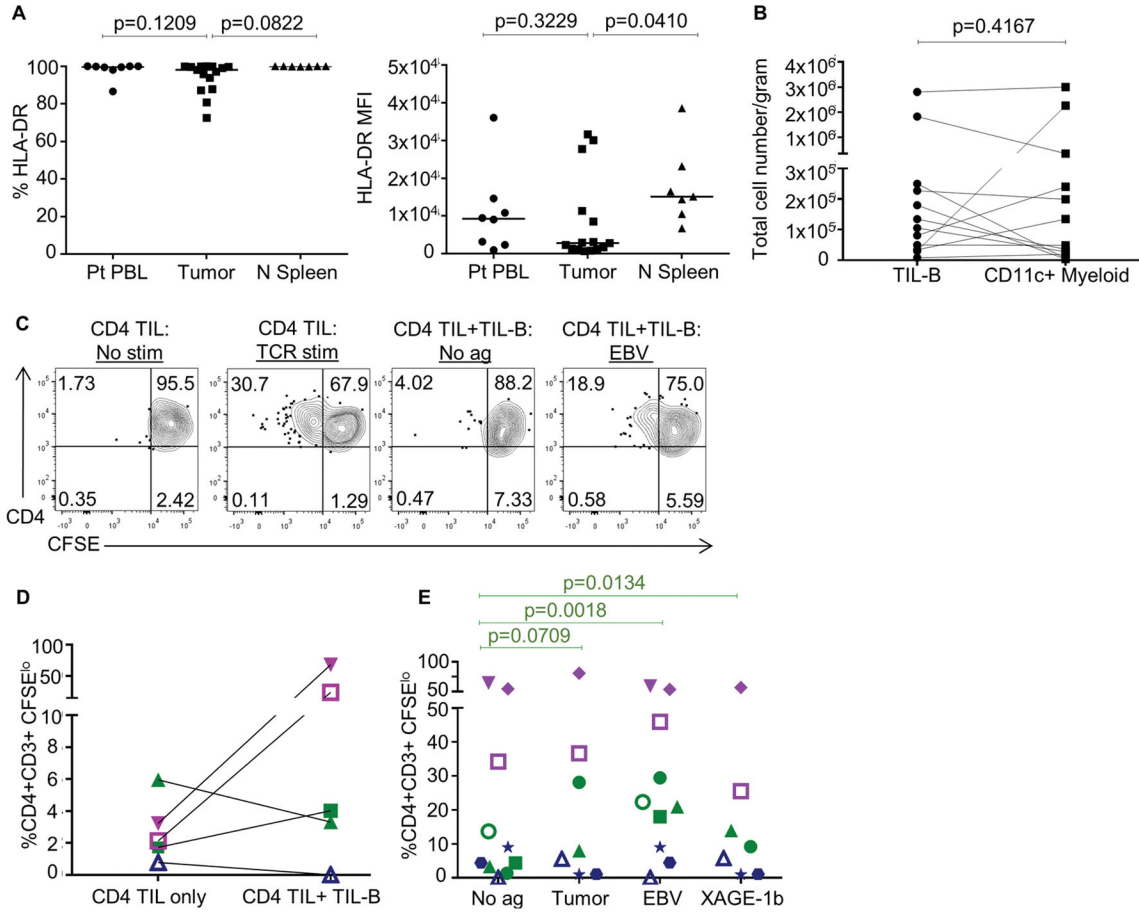
Fig. 4. TIL-Bs present antigen to CD4+ TILs in some NSCLC primary tumors

(**A**) HLA-DR expression on the indicated B cells is shown ($n = 7$–15). (**B**) Total numbers of TIL-Bs and DCs in NSCLC tumor samples is shown ($n = 12$). (**C**) Representative AP assays using NSCLC tumors are shown. (**D**) Comparison of CD4+ T-cell activated responses (purple), antigen-associated responses (green) and no responses (blue) in autologous AP assay in the absence of co-stimulation or exogenous antigen is shown ($n = 5$). (**E**) AP assay was performed in the presence of EBV lysate, autologous tumor lysate or XAGE-1b protein; each symbol represents a NSCLC patient sample ($n = 10$). *P* values are no antigen vs. tumor *P* = 0.0709, no antigen vs. EBV *P* = 0.0018, and no antigen vs. XAGE-1b *P* = 0.0134.
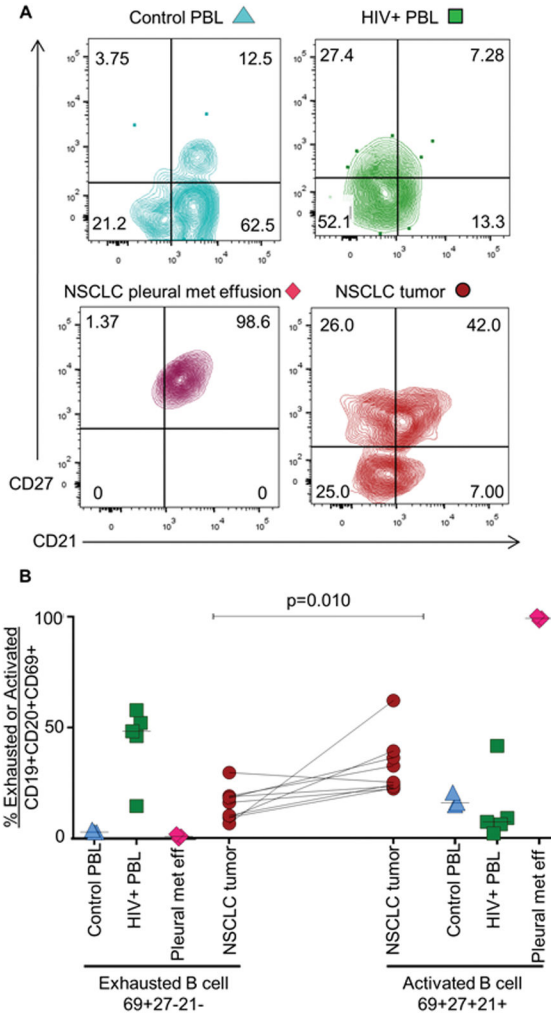
Fig. 5. TIL-Bs from NSCLC tumors have both an activated and exhausted phenotype
(**A**) Single-cell suspensions of NSCLC tumors were gated on live lymphocytes and stained with anti-CD19 and anti-CD20 to identify the TIL-B population and anti-CD69, anti-HLA-DR, anti-CD21, and anti-CD27 to quantitate the frequency of CD69+HLA−DR+CD21+CD27+ (activated) and CD69+HLA−DR+CD21−CD27− (exhausted) TIL-Bs. Control PBL, untreated HIV+ PBL, and effusions from NSCLC pleural metastases were used for comparison. (**B**) Data were compiled for frequency of activated and exhausted TIL-Bs in NSCLC patient tumors (n = 3–9). P value for exhausted vs. activated TIL-Bs = 0.010.
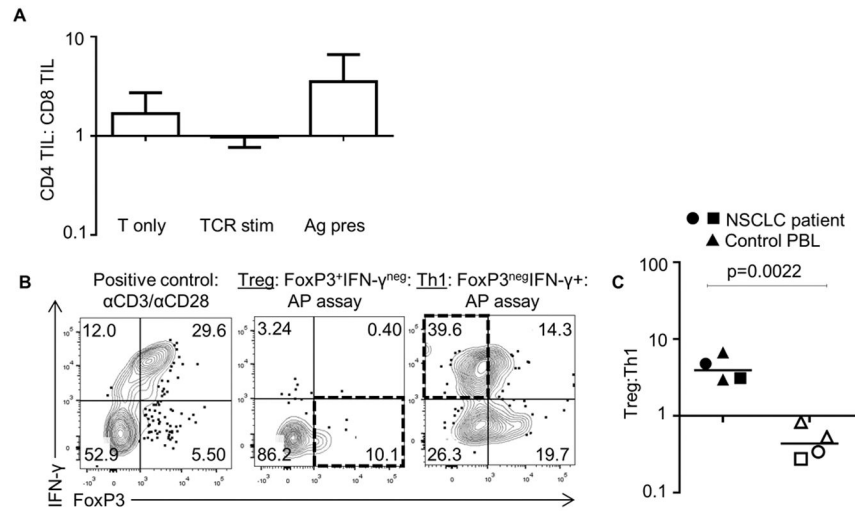
Fig. 6. TIL-B phenotype predicts CD4$^+$ TIL phenotype in NSCLC tumors
(**A**) CD4$^+$ and CD8$^+$ TIL frequencies were analyzed in AP assay; TIL without stimulation (T only), stimulation with plate bound anti-CD3 and soluble anti-CD28 (TCR stim), and autologous TIL-Bs and antigen are shown ($n = 3$–4). (**B**) Representative IFNγ and FoxP3 intracellular staining after AP assay. (**D**) Treg:Th1 populations were compared after AP assay in donors that had activated and exhausted B cells. Assay was performed as in Fig. 3, but with analysis of IFNγ and FoxP3 proteins. Closed symbols represent patients with exhausted TIL-B phenotype greater than 50% and dominant Treg phenotype at the end of the AP assay ($n = 4$). Open symbols represent patients with activated TIL-B phenotype greater than 50% and dominant Th1 phenotype at the end of the AP assay ($n = 4$). Triangle = control donor, square/circle=NSCLC patient. $P = 0.0022$ for Treg:Th1 log ratio.

Table 1

Summary of patient data

Survival key: NED = no evident disease, DOD = dead of disease.

Assay	Adenocarcinoma Squamous Cell Other	Age	Sex	Pathology	Previous or current smoker	Mutations	Survival
Flow cytometry	40 10 8	45–86	24 M 34 F	pT1a-pT4	52	3 KRAS mut 3 EFGR+ 3 TTF+ 2 p53 mut	Not known
Antigen presentation	9 1 0	56–71	4 M 6 F	pT1a-pT3	10	1 KRAS	2 NED 2 DOD
Total	49 (72.0%) 11 (16.2%)	--	--	--	62	--	--
% of Total	8 (11.8%)	--	--	--	91.2%	--	--